X-525-68-56

IONOSPHERIC DISTORTION OF MINITRACK SIGNALS IN SOUTH AMERICA

Tom Golden

February 1968

GODDARD SPACE FLIGHT CENTER
Greenbelt, Maryland

ABSTRACT

Records of tracking operations with the Minitrack system in South America have been compiled for a 12-month period. The number of passes scheduled and the number missed due to VHF propagation distortion have been computed in hourly increments beginning 1 July 1966. Records for STADAN tracking stations at Quito, Ecuador; Lima, Peru and Santiago, Chile show a diurnal maximum of interference close to local midnight and seasonal maxima during and immediately following the equinoxes. A similar compilation has been made of the incidence of spread echoes on ionosonde records made at nearby ionospheric sounding stations at Bogota, Colombia; Huancayo, Peru and Concepcion, Chile. A close diurnal and seasonal correlation between the NASA VHF interference data and the ESSA HF data is shown. The results of the study indicate a potential for ionospheric interference with satellite telemetry and command functions which must be performed instantaneously. Over a long period of time Minitrack orbit determination is not severely degraded by ionospheric distortion. A further examination of command and telemetry performance is recommended.

CONTENTS

IONOSPHERIC DISTORTION OF MINITRACK

SIGNALS IN SOUTH AMERICA

BACKGROUND

For many reasons, concern has been expressed recently about the effects of the ionosphere on operations with spacecraft in the VHF band at the three South American STADAN stations operated by Goddard Space Flight Center (GSFC). These stations are located close to the geomagnetic equator as shown in Table 1.

In the region near the geomagnetic equator, the phenomenon known as spread-F characteristically occurs. It is in this region that the Minitrack system which operates between 136 and 137 MHz has frequently experienced distortion of tracking signals by some propagation phenomena. Since equatorial spread-F is considered a nocturnal event, beginning soon after local sunset and continuing approximately till midnight and since the anomalous Minitrack behavior has been most evident in the evening hours the concensus is that Minitrack and spread echoes are due to the same distortion phenomena. Tracking difficulties have been observed more particularly in the fine (long baseline) antennas.[1] This portion of the Minitrack system is more sensitive to small phase changes than the ambiguity resolving (shorter baseline) antennas. Anomalies seem to predominate in the East-West baseline rather than the baseline disposed North to South. This is consistent with existing theories of plasma density alignment North to South along the magnetic field lines.

Operating procedures for the STADAN stations require that any anomalous tracking behavior for a satellite pass be reported daily. Anomalies due to propagation distortion are rather easily discriminated from other types of system interference by examining the analog phase records made in each Minitrack operation. Distortion due to propagation is thus easily recognized and reported on a daily basis. Reports in the files of teletype messages sent by the STADAN stations to GSFC contain records of Minitrack passes distorted by propagation effects. To obtain insight into the extent of the times of occurrence and the seasonal changes in propagation distortion of Minitrack in South America, a survey of these teletype reports on file has been made. A 12-month period beginning July 1, 1966, has been examined. As a crude basis for substantiation and correlation, ionospheric sounding records reported by the Environmental Science Services Administration (ESSA) for the same and prior periods have also been examined. ESSA publishes data from sounding stations which are relatively close to the STADAN sites as shown in Table 2.

The ESSA records which have been used for the present purposes are the hourly values of f_o F2. While these records are primarily designed to indicate the critical frequency of the ionosphere as viewed from the earth, the occurrence of any spread echoes by day and by hour of day is noted on each monthly record. The sounding frequencies reported in the ESSA data are below 25 MHz in all cases while the frequency of Minitrack operation is at VHF.

DATA FORMAT

Through the teletype messages to and from the STADAN stations, it is possible to determine the Minitrack pass schedule and the passes which were missed due to propagation distortion by day and by hour of day. Summaries of scheduled and missed passes have been compiled for each South American station. A typical schedule summary for Lima in February, 1967, is shown in Figure 1. The summary of passes missed during this same month is shown in Figure 2. The data by day contains an insufficient sample size to draw statistical conclusions so summaries by month were prepared for each station. The summaries have been made by hour of the day to indicate any trends toward nocturnal effects. The schedules for the 12-month period obtained from teletype messages to the station are shown in Figure 3 (a, b, c). These tables are representative of the samples from which anomalous propagation events were drawn.

MINITRACK PROPAGATION DISTORTION

Hourly Variation

The data on number of passes missed due to propagation distortion has been extracted from the teletype messages. It has been summarized for each month of the 12 months observed by hour of the day. Results are shown in Figure 4 (a, b, c). The data for the 12-month period has been totaled by hour of the day so that an annual picture of the hourly variation can be seen. A plot showing the percent of scheduled passes missed due to propagation distortion is shown in Figure 5. The most probable hour of occurrence lies between 0100 and 0900 hours GMT. For the South American STADAN stations, this corresponds to a local time beginning at 8:00 p.m. The chart hours indicated are ordinal hours, e.g., GMT hour from 11 to 12 is represented by value at 12 GMT.

Seasonal Variation

The monthly variation in schedule and misses caused by propagation can be obtained from the data in Figures 3 and 4. The percent of total passes missed due to propagation distortion in each month is shown in the curves of Figure 6. It can be seen here as in Figure 5 that Lima represents the worst interference problem with Quito and Santiago following in order. Lima missed an average of 8.2 percent during the 12-month period. The highest percentage missed on a monthly basis was 17.3 percent in November. Figure 6 shows a marked predominance of propagation distortion around the time of the equinoxes.

The yearly average for Quito is 2.5 percent of the scheduled passes missed due to propagation distortion. At Quito, the maximum was 8.2 percent of the passes missed during April. It is interesting to note that the November maximum observed at Lima is not present in the Quito data.

The average for the 12-month period at Santiago is 1.5 percent of the scheduled passes missed due to propagation distortion. At Santiago less than 5.2 percent of the total Minitrack passes were missed due to propagation distortion for any month of the year. This occurred during the month of March 1967.

To indicate the impact of propagation distortion on operations, histograms of the worst months for the three stations have been compiled. They are shown in Figure 7. It is evident that more than 90 percent of the passes during the worst hour were missed due to propagation distortion at Lima. At Quito it was 50 percent and at Santiago it was 25 percent. These are worst case conditions and are of interest because tracking, telemetry and command functions cannot be based on the best or average case.

IONOSPHERIC SOUNDING RESULTS

Hourly Variation

A similar treatment to that described above was given to the monthly ionospheric data obtained from ESSA sounding records. The total number of hours during which spread echo conditions were reported in the ionograms has been tabulated for each month for which data was available. Hour by month summaries of available data are shown in the Appendix (Figures A1 through A3). An hourly summary is shown in the curves of Figure 8 for each ESSA station. The preponderance of hours with spread echoes lies between 0100 and 1200 hours GMT (8:00 p.m. and 7:00 a.m. local time) similar to that seen in the Minitrack data of Figure 5.

Seasonal Variation

The hours of spread echoes as a percentage of total hours per month have been tabulated from the hourly value data and are plotted in Figure 9. Each station seems to have a similar characteristic. There are maxima around December for all three stations and minima around the month of June. This gives rise to a single cycle of spread echoes during a year as opposed to two cyclic changes seen in the Minitrack data (Figure 6).

STATISTICAL FACTORS

Data Sample Uniformity

An important factor in drawing conclusions from the available records is the uniformity of sampling times throughout each month. For the ESSA sounding data there is a regular schedule of measurements so that uniformity of sampling time distribution appears to be no problem. There are times, however, when sounding equipment is down for repair. The summary used here makes no attempt to correct for this lack of data. The treatment assumes no spread echo events in the soundings during the down time.

The time uniformity of the Minitrack schedule is typified by the operation record shown in Figure 1. The number of passes scheduled per hour throughout the year varied from zero to six. As to missing data, records for all but four days of the 12 months operation are available for Quito. One day's records are missing for Lima and none are missing for Santiago. Aside from these missing records there is no other down time for either tracking station except that required for scheduled maintenance.

The hourly schedules show a minimum number of 6 passes at 1100 hours GMT for Quito and at 2200 hours GMT for Lima (Figures 3a & b). The maximum number of passes during one month was 74. This occurred at 1400 hours GMT at Santiago (Figure 3c). The hours between 0100 and 1000 GMT contain a relatively large number of samples. The smallest number of passes scheduled during these hours in any month was 13 (Lima - 0300 hours - October).

Predictability

It should be emphasized that the trends by hour of day and season of year regarding Minitrack propagation distortion have been established without question by the analysis of the data available. For a more exact prediction of likelihood of ionospheric propagation distortion in STADAN it is necessary to have a better control of the sampling than at present. To obtain a good number for probability from the data presently available is not an easy matter. The difficulty arises from too much irregularity in the sample, i.e., the schedule for each station.

Several months of the schedule for the three stations have been studied for mean value, variance and standard deviation. Typical results are shown in Figures 10 and 11 (a, b). The deviation, σ, is approximately equal to the mean, $\bar{x}$, in each sample. This means that the likelihood of having no pass in a given hour (hence no measurement of distortion) is just about the same as the likelihood of having the average number or the maximum number of passes. To obtain a good number for the probability of missing a pass due to propagation distortion from such a varying sample is difficult if not impossible. What has been done for future operations is to arrange the station schedule so that at least one Minitrack pass each hour of the day is assigned providing the orbits of the spacecraft permit. Thus at least one sample per hour will be made and a firmer statistical basis for prediction will be attainable from future records.

DISCUSSION OF RESULTS

General

The hourly variation displayed in Figure 5 shows a preponderance of Minitrack propagation distortion centered around local midnight. The similar behavior of the ESSA ionosonde records in Figure 8 is strong evidence that the same phenomena is causing both results. There is a similar though less obvious correlation between the Minitrack records of Figure 6 and the ESSA records of Figure 9. The seasonal variation of Minitrack distortion at Lima and spread echo hours at Huancayo have been plotted in the same scale in Figure 12. Here a general agreement in the rate of increase and decrease can be seen in September and April, respectively. The Minitrack data, however, shows a minimum in January while the ESSA data shows an increase. An extensive analysis of this behavior is beyond the scope of the present report. However, the similarities of the two records are so notable that there is little question that both events are caused by the same or at least related phenomena.

Geographic Factors

In correlating ESSA and Minitrack data a natural question arises about the geographic separation between the two stations and whether ionospheric disturbances occurring over the STADAN site can be detected by the sounder some distance away. Kent and Koster from measurements made at 108 MHz[2] show the height of the base of the spreading to be between 150 and 210 miles. The vertically directed sounder antenna pattern varies significantly with frequency and azimuth angle.[3] Variation in beamwidths from 20 to 40 degrees is indicated.

The Minitrack antenna patterns are 11 by 76 degrees at the 3 db points.[4] At each STADAN site there is a pair of antennas arranged to obtain either equatorial or polar coverage. These crossed antenna patterns are shown in Figure 13. The relative location of STADAN and ESSA sounding stations is given in Table 2. Using the 210 mile height for the spreading phenomena given by Kent and Koster and assuming a sounder 3 db beamwidth of 20 degrees, a projection of the Minitrack and the sounder antenna patterns onto the ionosphere yields the overlap of antenna coverage shown in Figure 13. For convenience all three stations are shown. Only the Lima and Huancayo antenna patterns indicate a coverage of the same region in this analysis. The overlap appears predominantly in the polar Minitrack pattern.

The lateral extent of equatorial spread echoes has not been examined in detail. It is most likely true that a spread condition would prevail over the two stations. Pitteway and Cohen[5] have indicated that the location of the region of spread echoes cannot be determined by sounder antenna pattern coverage alone due to ducting in the ionosphere. He suggests that RF energy is trapped and propagates in a horizontal duct. Thus echoes might be seen at a considerable and usually undeterminable distance from the sounder.

Frequency Factors

Another factor which would tend to promote differences in the measurement or lack of correlation between the STADAN and the ESSA data is the five to one ratio of frequencies used. Since frequencies in the VHF band normally "penetrate" the ionosphere it is an interesting fact that there is any correlation at all with the spread echo phenomena measured by the ionosonde. The characteristic differences observed in Figure 12 cannot be explained at this time.

RECOMMENDATIONS

There are two kinds of reasons for being concerned about propagation distortion of VHF signals. First is the operational question, what is it doing to the function being performed, in the present case, tracking operations. Second is the question of increased scientific insight into the phenomena involved. An adequate answer to either of these questions is difficult and ramified. Since this paper is primarily concerned with Minitrack operation let us consider the impact of propagation distortion on the tracking function.

Minitrack data is used to determine orbital parameters. The traditional method of operation has not required that the system make a real time orbit determination. Phase measurements made by Minitrack are usually sent by teletype to GSFC for processing and orbit determination. Calculations are made some time after the data has been measured at the STADAN station. The loss of a Minitrack pass due to propagation anomalies means a loss of one set of data for orbit determination. There are, of course, "good" Minitrack passes for which there is no distortion. Experience shows the "good" passes have outnumbered the "bad" passes. The conclusion is that the Minitrack system as a whole has provided and will continue to provide very accurate orbital information despite propagation distortion.

The nature of telemetry and command systems, however, is not like that of Minitrack. The data presented in this study indicates that there are periods during which propagation distortion might degrade or cause a complete loss of telemetry information (Figure 7). Failure to get this information whether it is data to complete a scientific measurement in space or vital operational knowledge of spacecraft condition constitutes an unassessable monetary loss. Potentially, the command problem is even more critical. The command link is vital to the life of the spacecraft and the effectiveness of the whole project. Propagation interference with command signals can cause failures in the performance of any control function from orbital injection to spacecraft transmitter shut-down. While the conclusion of this effort is that Minitrack operation is not critically impacted by distortion there are other systems in which VHF propagation interference still poses important operational questions.

Oddly enough these operational questions cannot be fully resolved until more complete answers are available to the scientific questions. There are several important ionospheric characteristics about which more information is needed. First, a more accurate measure of the seasonal and diurnal dependence of distortion effects such as fading and scintillation is needed. The impact of fading on new modulation systems can then be estimated. Better statistics for telemetry and command operations in the equatorial region would be available. Scintillation measurements using the ATS-3 satellite and existing STADAN facilities should be thoroughly explored. To provide longer range predictions the measurements could be correlated with magnetic index, 10.7 cm solar flux and other cyclic phenomena.

Second, it is necessary that more data be obtained on correlation distance. It is well known that adequately separated antennas will exhibit different fading and interference characteristics because they will "look through" a different portion of the interfering medium. Space diversity techniques appear to offer an immediate solution to command or telemetry interference. VHF ionosphere correlation distance measurements are needed for the equatorial stations. The ATS-3 spacecraft and existing sites may again be useful for this purpose. To obtain an upper bound on distortion the worst location for making the measurements should be selected. The results of the Minitrack data presented here indicate that the STADAN site at Lima has the greatest interference level (Figures 5 and 6) and should be selected for the measurements.

ACKNOWLEDGMENTS

Appreciation is expressed to Mr. Rod Callies and to his staff of workers with the RCA Service Co. for their patient reading of the teletype messages. Support for their work supplied by the STADAN Operations Division is gratefully acknowledged. My thanks go also to Mr. C. A. White of the Antenna Systems Branch for his data compilation and reduction.

REFERENCES

1. Woodman, Ronald F., "Irregular Refraction of Satellite Signals Observed at Ancon, Peru." Presented at the Symposium of Space Research, Buenos Aires, Argentina, December 3, 1960

2. Kent and Koster, "Height of the Night-time F Layer Irregularities at the Equator," Nature 1961, Vol. 191, p. 1083

3. Cones, Cottony and Watts, "A 600 Ohm Multiple Wire Delta Antenna for Ionospheric Studies," CRPL-5-6, January 5, 1950

4. Lantz, P. A., "NASA Space Directed Antennas," Report X-525-67-430, September 1967, p. 7ff

5. Pitteway and Cohen, "A Waveguide Interpretation of 'Temperate Latitude Spread-F' on Equatorial Ionograms," Jour. of Geophys. Res., Vol. 66, No. 10, October 1961, p. 3141

Table 1

Coordinates of South American STADAN Stations

STADAN Site	Geomagnetic Latitude	Geographic Latitude	Geographic Longitude
Quito	22°N	1°S	79°W
Lima	0°	12°S	77°W
Santiago	30°S	33°S	71°W

Table 2

Coordinates of ESSA South American Sounding Stations

Site	Geomagnetic Latitude	Geographic Latitude	Geographic Longitude	Distance and Bearing from STADAN		
				Miles	Degrees	Site
Bogota	15°N	5°N	74°W	465	41°	Quito
Huancayo	0°	12°S	75°W	113	98°	Lima
Concepcion	25°S	37°S	73°W	272	208°	Santiago

LIST OF ILLUSTRATIONS

LIST OF ILLUSTRATIONS (Continued)

February 1967

GMT	1	2	3	4	5	6	7	8	9	10	11	12	13	14	15	16	17	18	19	20	21	22	23	24
1		1	2			3	1	2				2	2	2				3	3	2				
2	1	1		1	1	2	2		2	1			1	1	1	2	1	1	2		2	1		
3	1	2		2		1	3	2					1	1	2		2	3		2			1	
4	1		2		2	1	1		1			1			2	2	1	2	3		1	1		
5		1	3		1	1	2	2	2		1	1		1	1	1		2	3	3	1	1		1
6	1	1	1	1	3	2	2	2		1	1			2		2	2	4		1	1			
7	1	1	1		1	3	2	2	1		1			2	1		2						1	
8	2	1	2	1	1	1	1	4		1		1			1	1	1	1	1	1	1			
9	1	2	1	1	3																			
10		1		1		1		3		2	1			1	1	1	3	1	1	4		2		
11		2	1	1	1	3		1	1			1		2		1		2			1			1
12				2	2	1	2	1				1		1	1	1		1	4	1	1	1	1	1
13	1	1	1			1	1		1			1	1	1		1	2	4		1	2			1
14			1			2	3	1	1		1				1	3								1
15			1	2		2	1	2		1		1		2	1	2	3	1	3	1	2	1	1	
16		1	2	1	1	2	2		1	2				1		1		3			1	1		1
17				1		2	2	1	1	1	1			1			1	2	1	1	1	1		
18	1	1		2	1	1		1	2					1	2	1		3	2		2			
19			1		2	3	1	1	1				2		2		1	3	3	1				1
20		1	2	1	2				2	1					1		3				2			1
21	1	1	1	1	1	2	2	1		1				1	2	1	1							
22		1			2	1	1		2					1	2	1	2	4			1		1	
23		1	1		3	3	1	1	2				2	1				5			1	1		
24		1	3		1	2	2	2	1				1		3	1	2		3	1	1			1
25		2		1	2	1	1		2						1	1	2	1	1	1	1	2		
26	1	1		2	2	2	2	1	1					1	1		2	3	2	2	1			
27	1				2	1			1			1	1	2		1	3	1	2		2		1	
28		1	2	2	2	1		1		1			2	2							1	1		

Figure 1. Minitrack Pass Schedule for Lima for February 1967

February 1967 GMT	1	2	3	4	5	6	7	8	9	10	11	12	13	14	15	16	17	18	19	20	21	22	23	24
1						2	1																	
2						2	1																	
3				2			2	1																
4					1	1	1		1										2					
5						1																		
6					2	2	1																	
7					1	2	1																	
8																	1	1						
9				1	3																			
10		1		1		1		2		1														
11						1																		
12				1	1	1	2	1																
13						1	1		1															
14																								
15																								
16						1	2																	
17				1		1	1	1	1															
18				1					1															
19			1		1	2	1																	
20			2		1				2															
21				1		2	2	1																
22					2	1	1																	
23					2	3	1	1	1															
24																	1							
25				1	1	1	1																	
26				1	1	2	1																	
27																								
28						1		1																

Figure 2. Missed Minitrack Passes at Lima for February 1967

	GMT	1	2	3	4	5	6	7	8	9	10	11	12	13	14	15	16	17	18	19	20	21	22	23	24
1966	Jul	27	32	39	33	36	48	36	38	33	23	27	26	31	39	47	53	48	59	39	43	27	24	33	26
	Aug	21	25	43	30	29	37	27	33	13	18	23	16	21	34	46	39	34	37	27	29	24	26	24	23
	Sep	26	39	43	21	33	40	25	41	12	23	17	34	32	22	40	40	45	54	23	40	10	20	11	35
	Oct	33	39	39	27	20	46	34	57	49	32	19	15	27	40	46	31	21	43	25	55	40	38	20	20
	Nov	44	36	30	22	25	48	31	32	30	26	18	37	45	32	37	21	22	39	23	38	44	26	30	34
	Dec	20	18	40	21	21	38	38	29	39	48	46	31	17	22	38	17	29	35	36	38	33	42	44	30
1967	Jan	11	25	35	32	38	30	37	43	43	43	17	12	14	29	31	23	26	27	35	41	41	41	33	12
	Feb	15	25	41	30	33	44	40	29	25	13	9	6	12	19	35	27	32	43	48	33	27	12	9	12
	Mar	25	30	30	41	35	28	37	24	32	19	25	22	30	38	33	31	44	26	30	29	36	25	21	16
	Apr	31	49	48	47	28	32	40	50	41	31	41	30	32	46	54	43	30	40	39	40	41	52	31	26
	May	51	55	45	36	41	41	54	42	41	42	51	52	59	70	42	47	39	44	37	25	48	45	61	53
	Jun	32	41	41	40	48	46	42	51	49	64	65	47	37	52	48	47	40	38	53	47	47	63	58	43

Figure 3a. Monthly Minitrack Pass Schedule by Hour at Quito Beginning 1 July 1966

	GMT	1	2	3	4	5	6	7	8	9	10	11	12	13	14	15	16	17	18	19	20	21	22	23	24
1966	Jul	30	20	48	47	34	55	31	39	33	21	30	27	30	39	46	58	52	64	45	40	45	29	26	33
	Aug	15	28	44	28	33	38	26	33	13	25	28	19	19	36	49	30	29	45	37	28	13	26	17	21
	Sep	30	32	42	34	36	47	23	32	16	25	26	30	34	43	47	40	40	42	26	36	14	21	10	32
	Oct	31	52	42	13	23	43	39	50	43	33	25	14	27	46	49	24	17	53	27	52	44	46	21	26
	Nov	45	36	39	33	35	46	35	37	32	21	27	45	42	32	28	22	24	42	26	50	37	21	34	41
	Dec	29	28	38	19	37	43	39	33	52	44	47	32	21	30	33	18	40	45	32	34	38	39	39	33
1967	Jan	13	20	39	26	31	34	39	45	49	38	17	17	13	31	30	24	19	25	26	36	41	33	16	13
	Feb	13	25	28	23	36	45	36	31	26	13	7	10	14	30	26	26	36	52	35	26	26	12	6	12
	Mar	26	21	32	33	44	35	40	33	31	22	22	30	21	37	37	43	42	32	31	35	42	20	22	16
	Apr	32	45	37	37	37	37	39	39	34	35	33	29	38	43	51	48	33	33	41	35	38	46	30	19
	May	46	57	41	36	37	54	32	30	39	33	48	40	52	66	41	40	42	40	42	32	39	30	53	45
	Jun	35	45	31	35	46	42	37	42	37	58	44	38	43	42	38	36	29	39	39	43	35	56	53	38

Figure 3b. Monthly Minitrack Pass Schedule by Hour at Lima Beginning 1 July 1966

	GMT	1	2	3	4	5	6	7	8	9	10	11	12	13	14	15	16	17	18	19	20	21	22	23	24
1966	Jul	35	30	50	48	58	35	27	29	30	26	37	39	49	64	74	56	63	74	59	64	43	33	41	36
	Aug	28	49	47	41	43	33	39	34	39	37	21	23	35	52	42	32	48	43	27	40	23	36	22	13
	Sep	23	41	38	43	51	36	40	31	15	21	42	37	48	53	44	51	48	52	39	35	17	18	19	26
	Oct	46	43	51	22	44	46	54	65	46	33	16	29	45	53	35	22	24	40	40	53	51	45	33	38
	Nov	34	42	49	39	61	42	56	45	35	29	42	46	39	45	24	17	28	40	27	39	51	49	42	51
	Dec	28	34	38	29	50	46	58	43	45	43	51	29	28	41	30	33	43	43	35	36	40	45	42	31
1967	Jan	26	38	48	43	38	34	52	54	53	33	12	13	27	36	28	24	21	37	47	54	57	41	23	22
	Feb	16	19	23	37	61	54	41	31	20	15	20	16	26	26	25	27	31	43	35	17	25	20	15	16
	Mar	31	39	45	58	49	35	33	35	17	20	23	27	38	35	43	44	38	38	50	45	47	36	32	35
	Apr	39	39	47	38	61	43	46	40	42	29	48	43	57	59	45	45	39	44	41	43	41	38	31	18
	May	29	58	28	28	37	34	25	47	48	36	40	50	47	60	37	35	23	39	33	34	33	42	53	46
	Jun	32	38	35	33	59	40	39	39	39	42	39	19	31	32	33	31	29	37	39	50	58	66	51	37

Figure 3c. Monthly Minitrack Pass Schedule by Hour at Santiago Beginning 1 July 1966

	GMT	1	2	3	4	5	6	7	8	9	10	11	12	13	14	15	16	17	18	19	20	21	22	23	24
1966	Jul															1									
	Aug													1				2		2	1	1	1		
	Sep			2	4	2	5		1				1	1											
	Oct		5	6	4		1		2		1										1				
	Nov			1	1		3	2		2															
	Dec						1			1		1													
1967	Jan			1	2	4	2	2		1		1													
	Feb			1	9	9	12	7	3										1	1					
	Mar		1	6	19	15	8	6	3																
	Apr		5	24	19	8	8	5	2																
	May			1	1	2						1													
	Jun				1	1	1																		

Figure 4a. Minitrack Passes Missed by Hour Due to Propagation at Quito

	GMT	1	2	3	4	5	6	7	8	9	10	11	12	13	14	15	16	17	18	19	20	21	22	23	24
1966	Jul			1	5	3	1	1		2		1													1
	Aug			4		1	1			1		3	1												
	Sep		4	14	7	8	12	1	5	1	2	1	3		1										
	Oct		8	28	7	15	25	17	11	5	5	3		1											
	Nov		4	11	19	25	43	19	12	4	2	4	1												
	Dec		2	3	5	12	15	11	8	8	7	4						1							
1967	Jan			10	5	11	11	10	4	3	2				1										
	Feb		1	3	10	16	28	20	7	7	1							2	1	2					
	Mar		1	12	13	24	24	19	11	1		1													
	Apr		6	18	21	14	13	4	3																
	May			2		4		2	1	1	3		2							1		1			
	Jun			2	1	4	1	1	1			2		1						1					

Figure 4b. Minitrack Passes Missed by Hour Due to Propagation at Lima

	GMT	1	2	3	4	5	6	7	8	9	10	11	12	13	14	15	16	17	18	19	20	21	22	23	24
1966	Jul			1																			1		
	Aug				2	1															2				
	Sep					1	1							1	1										
	Oct			2				1					1		1					1					
	Nov							1	2																
	Dec				1						1				1			1							
1967	Jan			2	2	5	5	6	4	7	2	1					1				1				
	Feb				5	11	5	2	2	1		1			1				1	2	1				
	Mar		1	4	11	12	6	3	5		1		1				1					1			
	Apr		5	2	2	6	5	2	1																
	May																								
	Jun		1																						

Figure 4c. Minitrack Passes Missed by Hour Due to Propagation at Santiago

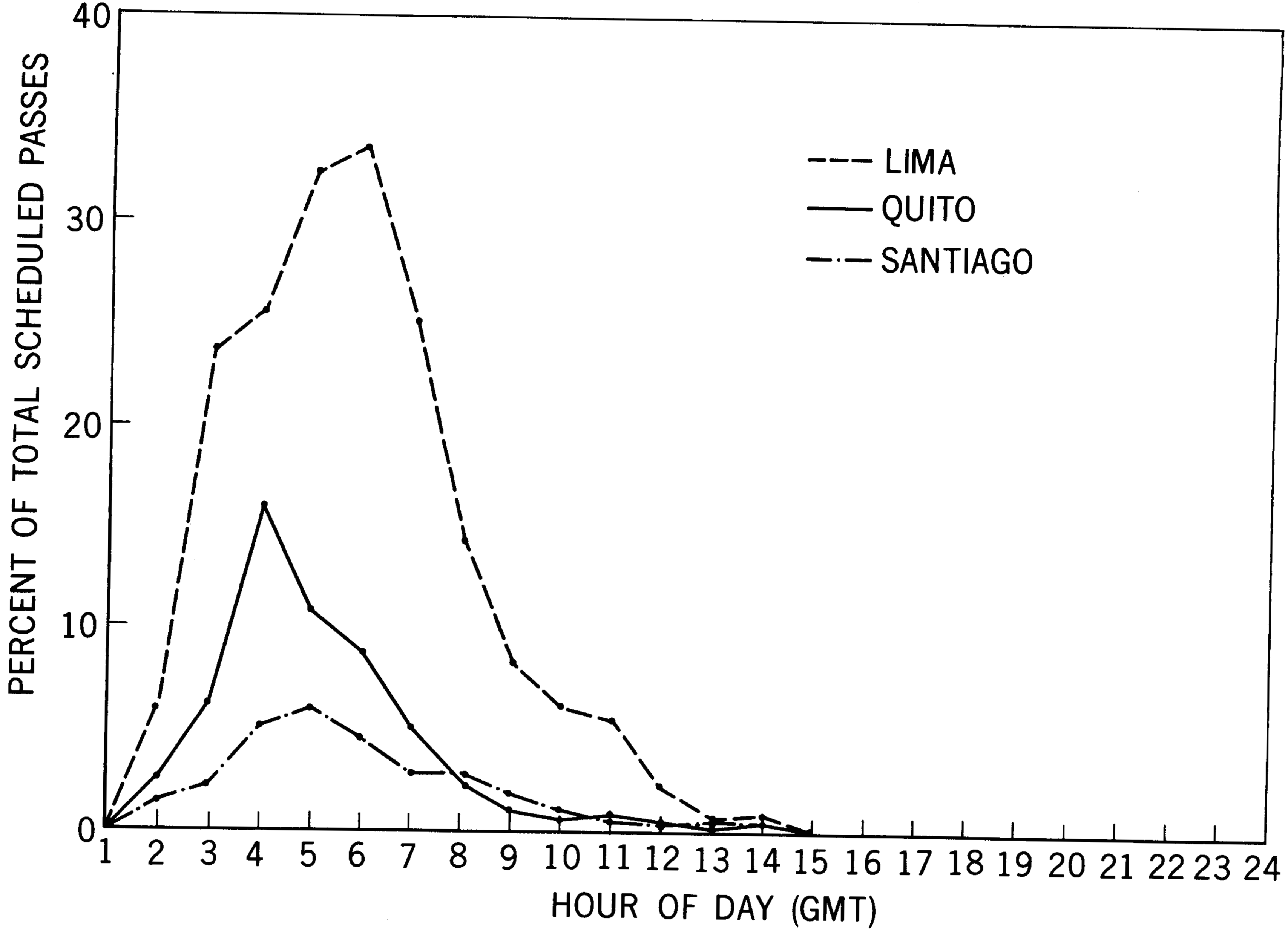

Figure 5. Scheduled Minitrack Passes Missed Due to Propagation Distortion by Hour of Day for 12 Months

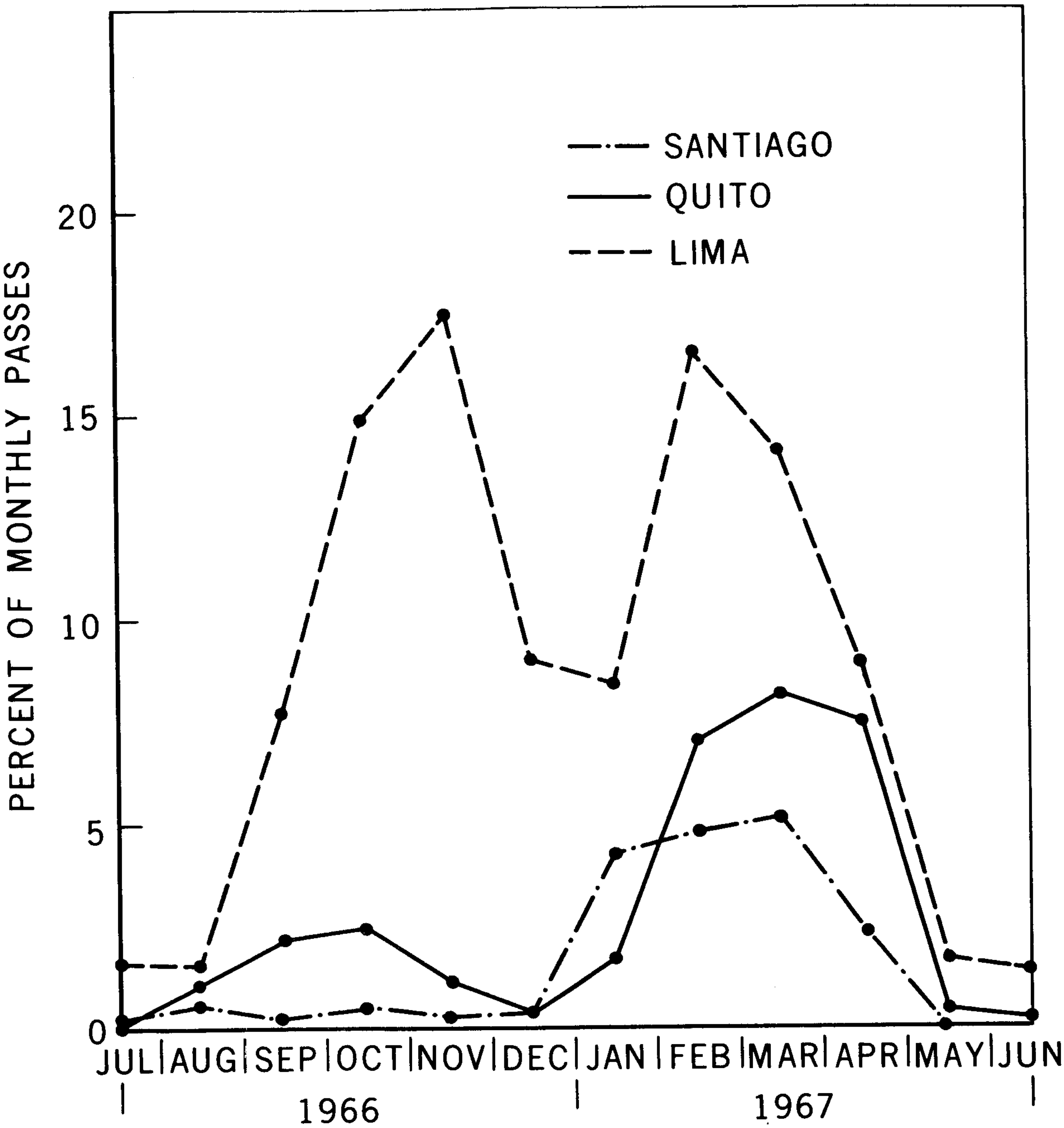

Figure 6. Scheduled Minitrack Passes Missed by Month Due to Propagation Distortion

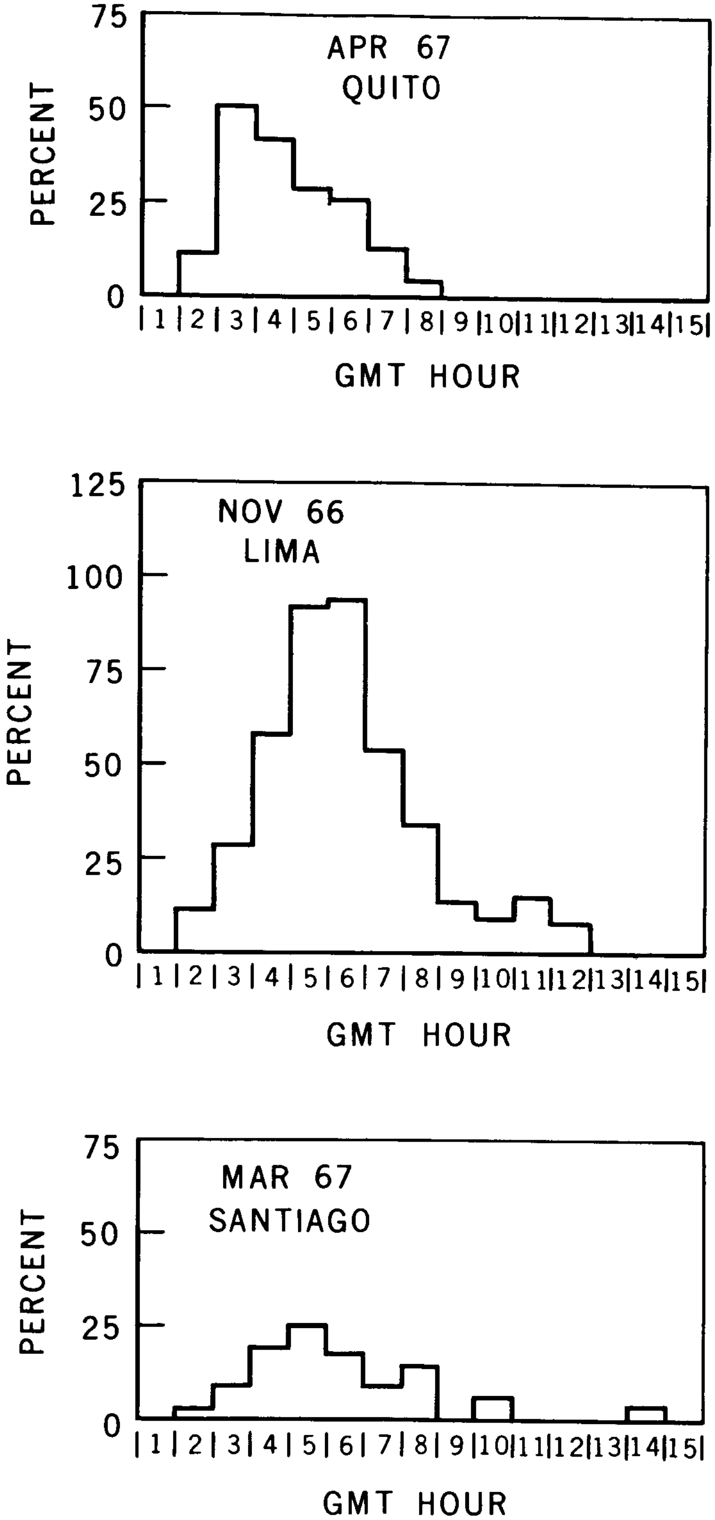

Figure 7. Percent of Scheduled Passes Missed for the Worst Month by GMT Hour

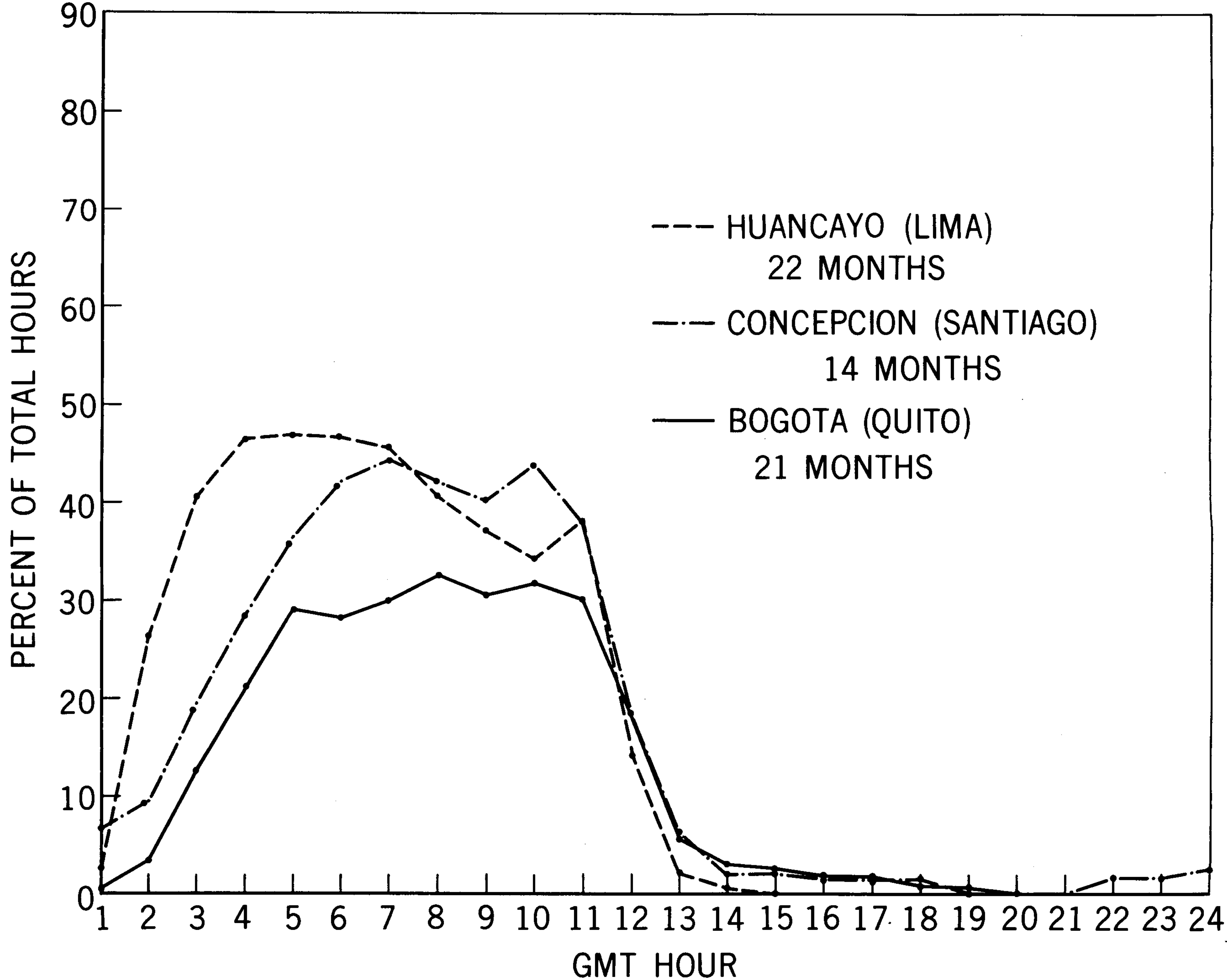

Figure 8. Percent of Total Hours by Hour in which Spread Echoes were Reported

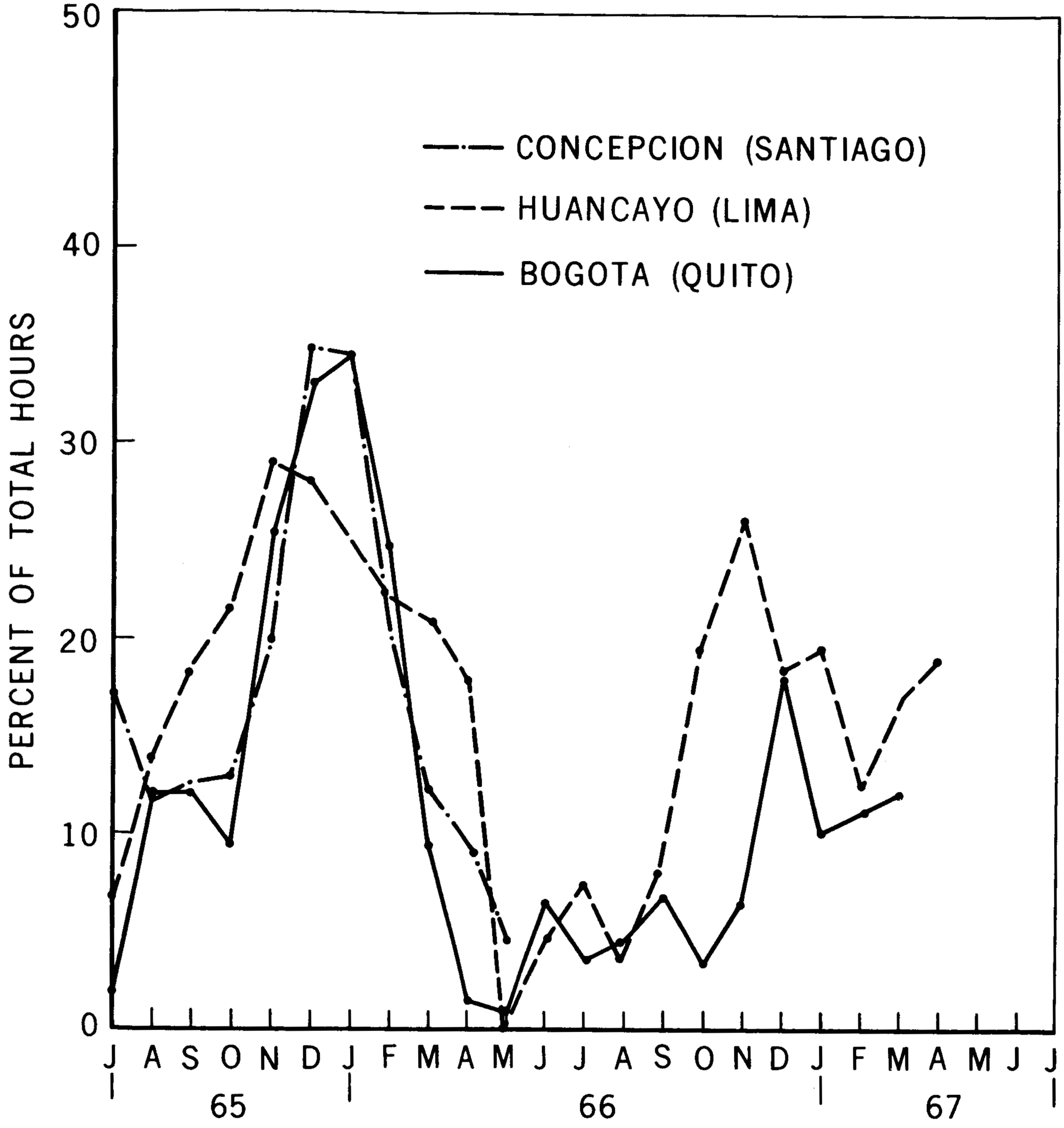

Figure 9. Percent of Total Hours by Month in which Spread Echoes were Reported

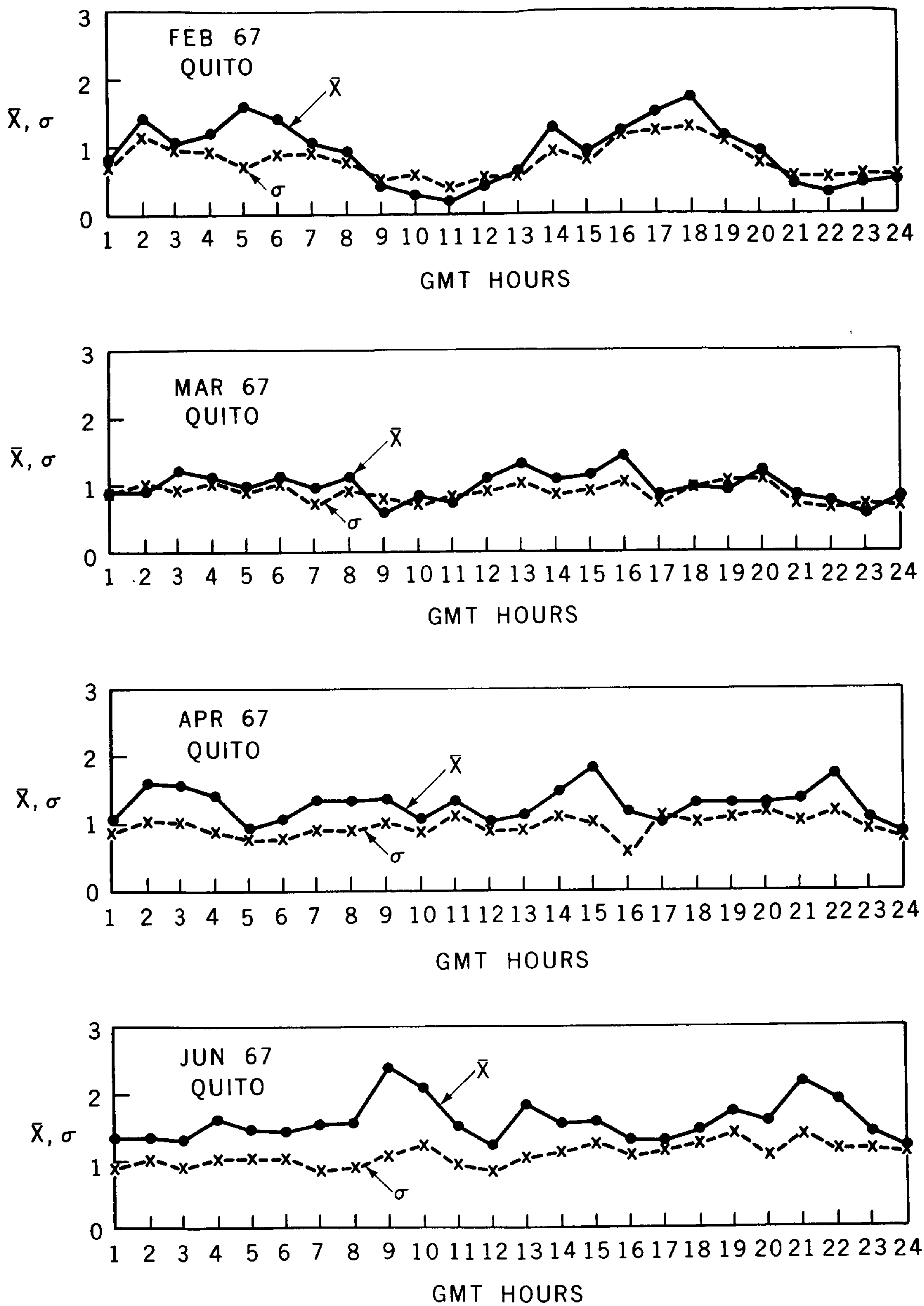

Figure 10. Mean Value and Deviation of Pass Schedule During GMT Hour for Selected Months at Quito

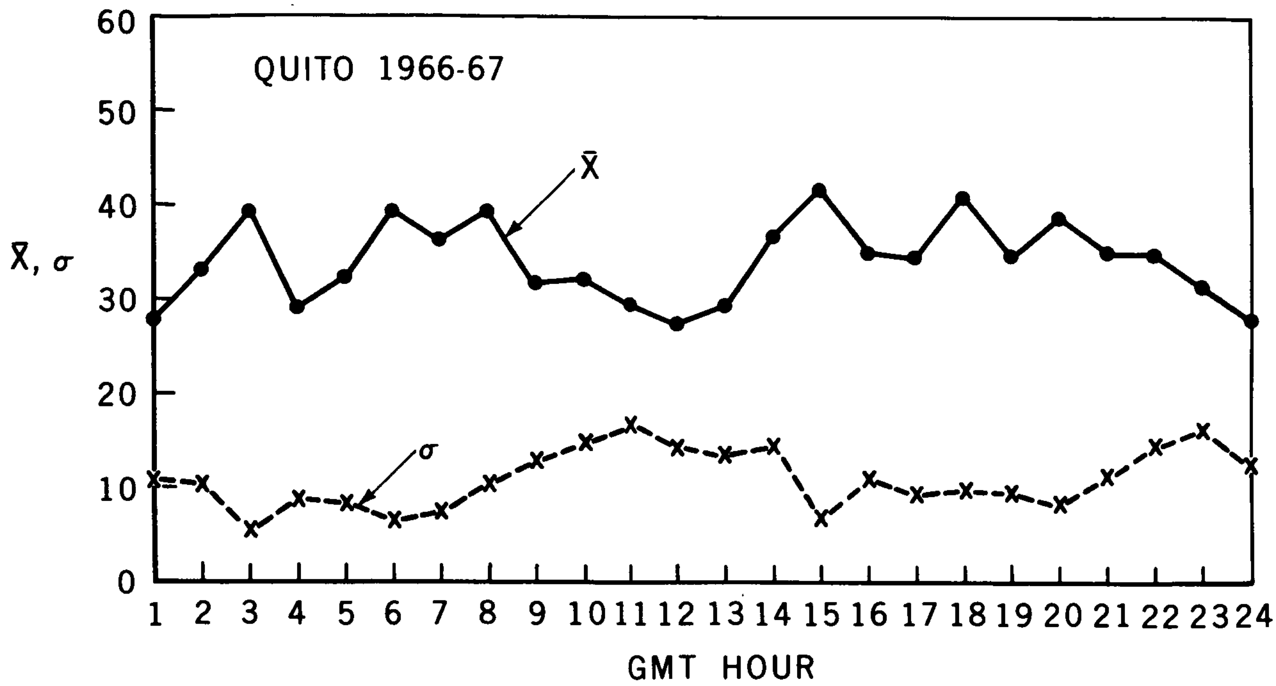

Figure 11a. Mean Value and Deviation of Monthly Pass Schedule by GMT Hour for 12 Months at Quito

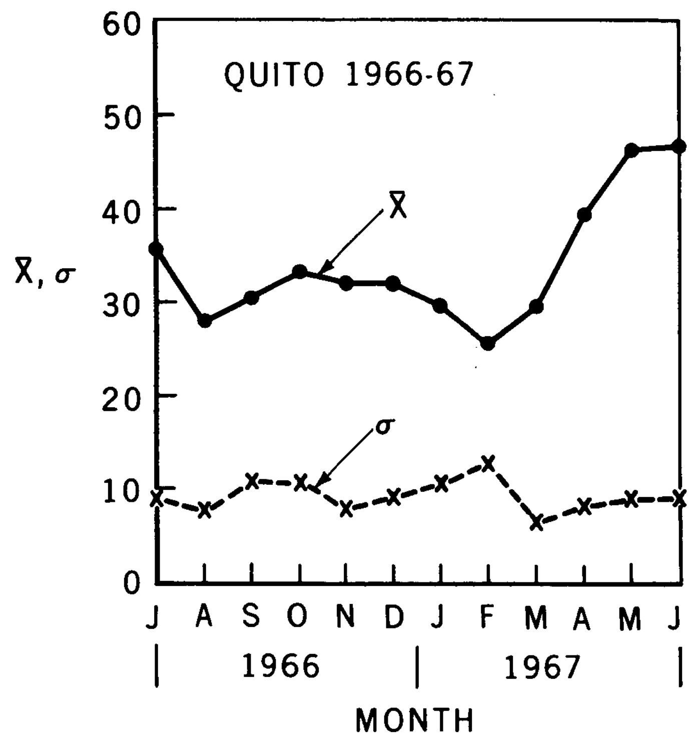

Figure 11b. Mean Value and Deviation of Pass Schedule by Month for Total Passes in Month at Quito

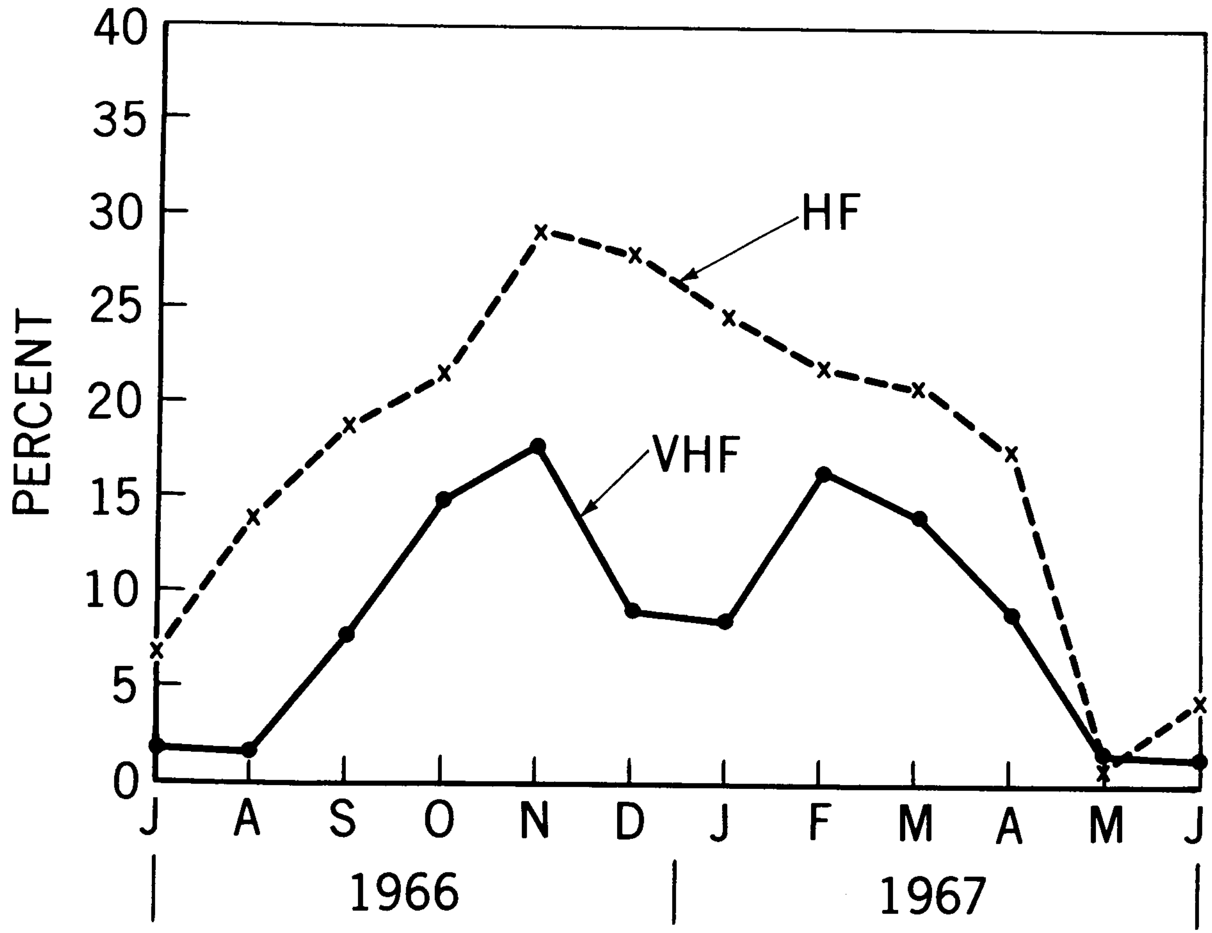

Figure 12. Percent of VHF Minitrack Passes Missed and of Total Hours in which HF Spread Echoes were Reported

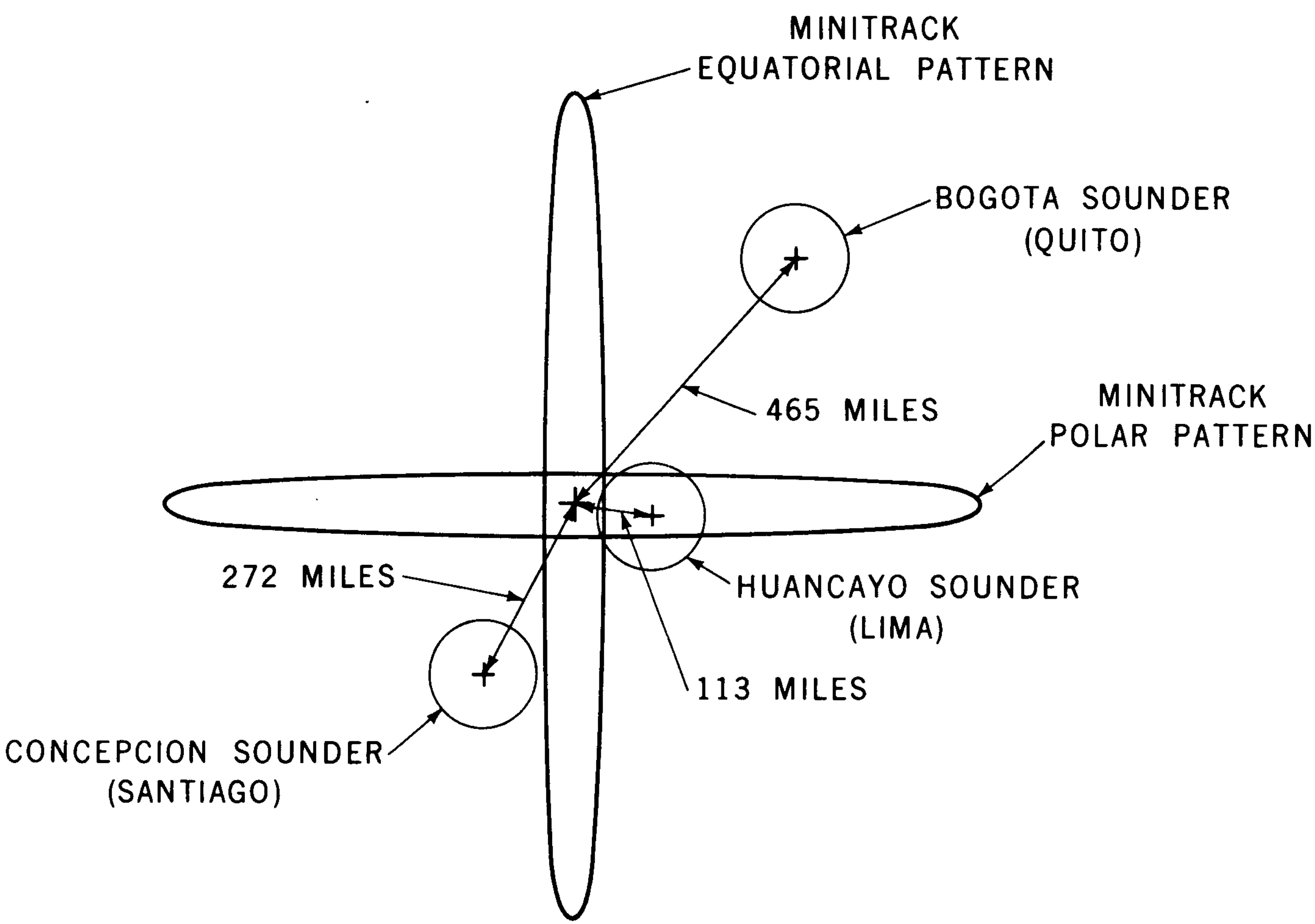

Figure 13. Projection of 3 db Antenna Pattern Contours on Ionosphere at Height of 210 Miles

	GMT	1	2	3	4	5	6	7	8	9	10	11	12	13	14	15	16	17	18	19	20	21	22	23	24
1965	Jul					1	2	3	2	3	3														
	Aug			1	2	7	11	15	13	12	10	6	3		2	2	2		2	1					
	Sep		1	1	5	6	8	10	11	10	10	9	9	2	1	2	1	2							
	Oct			2	4	9	11	8	11	7	7	8	2	1											
	Nov		5	9	12	19	18	21	21	20	22	19	9	5	1			1							
	Dec		4	11	19	25	25	25	25	28	27	28	19	5	2	1		1							
1966	Jan	2	4	16	25	24	26	26	27	26	28	24	21	1	2	3	1								
	Feb		2	6	11	18	18	18	20	17	21	21	12	1										1	
	Mar			2	2	7	8	10	9	9	9	9	4	1											
	Apr						1			1	4	3	1												
	May							1	1		1	2							1	1					
	Jun						1	2	5	7	6	6	3	1	4	3	3	3	2	1					
	Jul			1	1		1	2	3	3	4	2	3	2	1	1	1	1							
	Aug		1	2	1	1	1		1		2	3	4	4	4	4	4	2							
	Sep			3	4	4	6	3	6	4	6	7	3	2	1				1						
	Oct			2	3	4	2	1	1	2	1	5	2	1	1										
	Nov			1	3	3	5	7	8	5	5	7	4	1											
	Dec			3	8	13	10	14	19	16	19	20	7	2	1	1		1							
1967	Jan			2	9	9	8	11	9	9	6	6	3	3											
	Feb		1	4	9	9	5	7	9	9	8	6	5	2											
	Mar		4	16	16	16	12	7	6	6	3	1	1	1											

Figure A-1. Spread Echo Conditions at Bogota, Columbia – Total Hours Having Event by Hour and Month

	GMT	1	2	3	4	5	6	7	8	9	10	11	12	13	14	15	16	17	18	19	20	21	22	23	24
1965	Jul					2	2	5	7	5	5	12	11												
	Aug		1	6	8	10	9	9	12	12	14	14	9												
	Sep	2	13	17	14	13	11	13	11	9	12	15	5												
	Oct		12	17	22	17	18	19	16	12	10	13	3	1											
	Nov	2	14	14	19	23	25	24	22	23	19	21	3												
	Dec		7	14	23	25	29	26	23	24	20	17													
1966	Jan	1	3	12	16	17	23	23	24	22	22	18	5												
	Feb		7	16	15	20	20	21	18	13	11	5		1	1										
	Mar		14	19	20	20	18	18	11	9	8	8	9	2	1										
	Apr		7	16	21	19	14	12	10	8	8	8	6												
	May			1		2	1				1	1													
	Jun		1	1	2	3	3	2		4	5	5	6												
	Jul		3	8	8	6	3	4	4	5	6	7	1												
	Aug		2	2	2	1		2	2	2	3	5	4												
	Sep	1	5	6	6	5	4	3	3	6	5	7	6	3	1										
	Oct	6	18	19	22	20	15	13	11	10	8	6	4	3	1										1
	Nov	2	14	19	24	24	26	25	21	16	10	5	2	1											
	Dec		8	20	24	26	29	28	29	27	24	18	5												
1967	Jan		8	14	15	16	19	19	17	14	11	9	3												
	Feb		6	10	11	11	10	10	8	8	5	2	2												
	Mar		17	23	21	18	20	17	11	6	6	5	4												
	Apr	2	16	16	17	16	10	11	10	11	14	7	6	1											

Figure A-2. Spread Echo Conditions at Huancayo, Peru - Total Hours Having Event by Hour and Month

	GMT	1	2	3	4	5	6	7	8	9	10	11	12	13	14	15	16	17	18	19	20	21	22	23	24
1965	Jul	2	3	5	6	11	15	13	14	12	12	13	10	3		1		2	2	1		1	1		1
	Aug	2	2	3	5	6	10	10	10	11	9	7	9										1	1	1
	Sep		1	1	3	8	14	12	14	13	14	12	1												
	Oct		1	3	8	10	12	12	11	10	14	13	1	1											
	Nov	3	6	8	10	15	16	16	17	14	19	11	5	3					1				1	1	1
	Dec	4	7	14	21	26	23	29	24	24	27	21	14	7	4	4	3	2	1			2	1		2
1966	Jan	6	8	18	26	27	25	27	25	24	24	23	13	7	2	1		1	1						1
	Feb		3	9	10	16	16	17	15	18	15	15	3		1	1	1								
	Mar	2	1	3	3	7	12	14	12	9	15	11	2												
	Apr	3	4	4	4	6	8	8	7	6	7	4	4										2	1	2
	May	2		4	4	2	1	2	3	3	2	5	2					1			1			2	
	Jun																								
	Jul																								
	Aug			1	4	3	2	2	2	3	2	2	3	2		1	1								
	Sep																								

Figure A-3. Spread Echo Conditions at Concepcion, Chile – Total Hours Having Event by Hour and Month